METROLOGY AND MEASUREMENT SYSTEMS
VOL. XIV, NUMBER 4 (2007)

JERZY AUGUSTYN

Kielce University of Technology
Faculty of Electrical, Automatic Control and Computer Engineering
e-mail: etmja@tu.kielce.pl

INFLUENCE OF THE STRUCTURE OF SIGNAL CONDITIONING CIRCUITS ON THE UNCERTAINTY OF IMPEDANCE MEASUREMENT WITH ALGORITHMIC METHODS

The article presents an estimation of the impedance measurement uncertainty determined in the measurement circuit with a two-channel sampling transducer. Using the Monte Carlo method, the influence of dynamic error and quantization error on the probability distribution of the impedance components error has been analysed. Comparison of these errors propagation has been made for three structures of conditioning circuits of voltage and current signals on measured impedance. On the basis of the obtained probability distribution, the value of the expanded uncertainty of impedance components has been determined.

Keywords: uncertainty, conditioning circuits, measurement of impedance components, measurement algorithms

1. INTRODUCTION

Application of measurement circuits with analog-to-digital processing enables to use appropriate digital processing algorithms of sampled measurement signals to determine the values of impedance components [1–7]. There are many processing algorithms used while feeding the measured impedance with sinusoidal voltage or current. In order to determine the instantaneous values of voltage and current in the measured impedance, a two-channel data acquisition system with simultaneous sampling in both channels should be used. Additionally, the processing algorithms are simplified in synchronous sampling conditions with the frequency of the generator that feeds the measured impedance. For initial processing of the current flowing in the measurement circuit into voltage, a standard resistor in series or active I/V converter are used [1–7]. Additionally, the values of converted signals should be properly scaled depending on the range of the A/D converters in use. The calculation of impedance component values should be then preceded by an appropriate reconstruction algorithm of instantaneous values of voltage $u(t)$ and current $i(t)$ on the measured impedance $\underline{Z} = R + \mathrm{j}X$.

A block diagram of the measurement circuit, that takes into account the presented basic processing steps, is shown in Fig. 1.

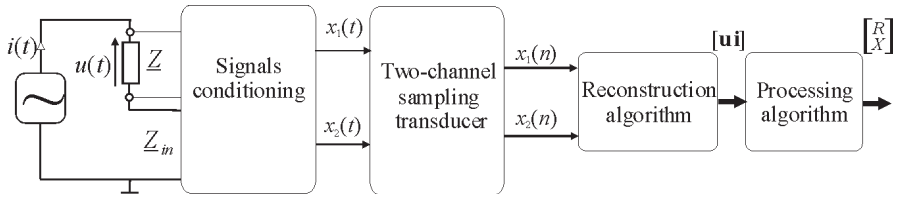

Fig. 1. Block diagram of the circuit for impedance component calculation.

Depending on the applied structure of conditioning circuits, the form of reconstruction algorithms is subject to change. Due to the fact that the input circuit structure must be taken into consideration, their mathematical models forms are also different, which as a consequence can have a significant influence on probabilistic properties of the measurement errors.

Apart from the errors introduced by conditioning circuits of voltage and current, during estimation of the uncertainty of final measurement result one should also consider the errors resulting from the application of sample/hold circuits as well as analog-to-digital converters [6, 8–9]. Moreover, due to the approximate form of dependencies describing the way of processing sequences of quantized samples, the processing algorithms introduce an additional measurement error. Thus, the output quantities vector $\mathbf{y} = [R,\ X]^{\mathbf{T}}$, calculated in accordance with the assumed processing algorithm, contains errors which are the consequence of composing both the errors of the sampling transducer propagated through successive elements of the processing channel and own errors of the algorithm.,

For the successive instants $n = 0, 1, ..., N - 1$, the reconstruction algorithm can be described by the matrix equation

$$\left[\ u(n),\quad i(n)\ \right] = \left[\ x_1(n),\quad x_2(n)\ \right]\mathbf{T}, \tag{1}$$

where $x_1(n)$, $x_2(n)$ are the analog-to-digital processing results, $u(n)$, $i(n)$ are the pair of reconstructed values of voltage and current, and $\mathbf{T}$ is the 2×2 – dimensional transformation matrix with elements depending on the structure of the conditioning circuits of voltage and current [5–6].

The processing algorithm is given as a matrix equation

$$\begin{bmatrix} R \\ X \end{bmatrix} = \mathbf{F}(\ \mathbf{u}\quad \mathbf{i}\ ). \tag{2}$$

where the column vectors $\mathbf{u}$ and $\mathbf{i}$ contain the reconstructed values of voltage and current, and R, X are the calculated impedance components.

One of the methods that enables the estimation of measurement uncertainty in the circuit composed of a sampling transducer and the processing algorithm is the application of probability distribution propagation rule as the basis for uncertainty determination. For this purpose the Monte Carlo method is applied, using a mathematical measurement model [8–12]. In this paper the influence of the structure of conditioning circuits of voltage and current on the probabilistic properties of the impedance component measurement results has been analysed.

2. RESULTING ERRORS OF SINGLE SAMPLE PROCESSING IN THE TWO-CHANNEL SAMPLING TRANSDUCER

Each of the two channels of the sampling transducer processes the instantaneous values of voltage $u(t)$ or current $i(t)$ connected with the measured impedance $\underline{Z}$ into sequences $\{x_1(n)\}$ and $\{x_2(n)\}$ of the output signal values of the A/D converters, determined at the sampling instants $n = 0, 1, ..., N-1$. The basic error components appearing at the output of such a converter are related to the dynamic properties of the conditioning circuit and the quantization process [8–9].

As the frequency band of the operational amplifiers used in the conditioning circuits is limited, there are three basic types of circuits (Fig. 2) differing in their dynamic properties.

The description of dynamic properties of the sampling transducer is most frequently assumed as a first-order linear differential equation. In the case of voltage channels (with differential or single-ended input) its spectral transmittance can be modelled by

$$\underline{K}_i(\mathrm{j}f) = \frac{K_{0i}}{1 + \mathrm{j}\frac{f}{f_{gi}}}, \tag{3}$$

where K_{0i} is the static sensitivity and f_g is the cut-off frequency of the amplifier in i^{th} processing channel ($i = 1, 2$).

After taking into account the gain bandwidth product f_T, which describes the frequency properties of operational amplifier, Eq. (3) is given as

$$\underline{K}_i(\mathrm{j}f) = \frac{K_{0i}}{1 + \mathrm{j}\frac{f}{f_T}K_{0i}}. \tag{4}$$

The result of the transmittance form (4) is the value of the complex dynamic error at the output of the sampling transducer

$$\underline{\Delta}^d_{xi}(\mathrm{j}f) = \underline{\tilde{X}}_i(\mathrm{j}f) - \underline{X}_i(\mathrm{j}f) = -\underline{U}_i\frac{\mathrm{j}\frac{f}{f_T}K_{0i}^2}{1 + \mathrm{j}\frac{f}{f_T}K_{0i}}, \tag{5}$$

where the value of the output signal of the sampling transducer with dynamic error is marked with a tilde, $\underline{X}_i(\mathrm{j}f)$ is the complex value of the output signal of an ideal transducer (with unlimited frequency band), and $\underline{U}_i$ is the complex value of the input voltage of i^{th} sampling transducer channel.

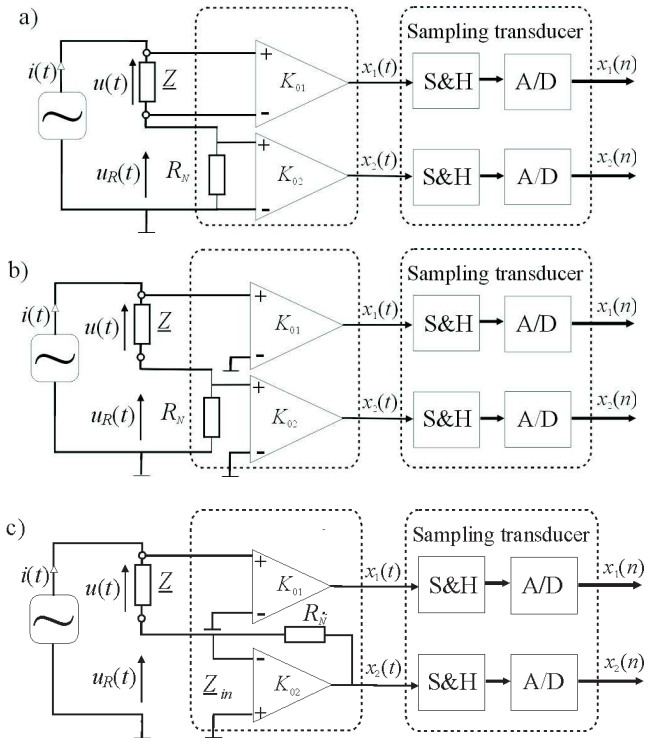

Fig. 2. Structure of the signals conditioning circuits: with series resistor and two voltage channels with differential inputs (a), with series resistor and two voltage channels with single-ended inputs (b), with one voltage channel with single-ended input and active I/V converter (c).

If the active converter is used in the current channel (Fig. 2c), the corresponding transmittance can be presented as

$$\underline{K}_2(\mathrm{j}f)_c = -\frac{R_N}{1+\mathrm{j}\frac{f}{f_T}}, \tag{6}$$

and the value of the dynamic error is then equal to

$$\underline{\Delta}^d_{x2}(\mathrm{j}f)_c = \underline{I}R_N\frac{\mathrm{j}\frac{f}{f_T}}{1+\mathrm{j}\frac{f}{f_T}}, \tag{7}$$

where R_N is the static transresistance of the I/V converter, $\underline{I}$ is the complex value of current flowing through the measured impedance, and subscript c denotes the conditioning circuit presented on Fig. 2c.

Simultaneously, in case of using an active I/V converter, in the measurement model one should consider its input impedance

$$\underline{Z}_{in}(\mathrm{j}f)_c = R_N \frac{\mathrm{j}\frac{f}{f_T}}{1+\mathrm{j}\frac{f}{f_T}}, \tag{8}$$

which influences the value of the dynamic error in the voltage measurement channel.

For sinusoidal signals, the dynamic error in the time domain can be shown as

$$\Delta^d(t) = E_d \sin(\omega t + \varphi_d), \tag{9}$$

where: $E_d = |\underline{\Delta}^d(\mathrm{j}f)|$ and $\varphi_d = \mathrm{arctg}\dfrac{\mathrm{Re}\{\underline{\Delta}^d(\mathrm{j}f)\}}{\mathrm{Im}\{\underline{\Delta}^d(\mathrm{j}f)\}}$.

If the sampling instant of measured waveforms is selected randomly from the population with uniform distribution, the probability density function (PDF) of the dynamic error of a single processing result of instantaneous signal values in every channel of the sampling transducer is described by the bimodal function

$$g\left(\Delta^d_{xi}(t)\right) = \frac{1}{\pi\sqrt{E^2_{di} - \left(\Delta^d_{xi}(t)\right)^2}}. \tag{10}$$

Application of the reconstruction algorithm (1) can lead to correlation of reproduced signals of voltage and current [5]. Probabilistic properties of a single processing result is then described by joint PDF of random vector $[u, i]$: $g_{[u,i]}(x_1, x_2)$.

For each of the analysed structures of the conditioning circuit the corresponding dynamic error vector can be constructed:

$$\left[\ \underline{\Delta}^d_{x1},\ \ \underline{\Delta}^d_{x2}\ \right] = \left[\ \tilde{\underline{X}}_1(\mathrm{j}f),\ \ \tilde{\underline{X}}_2(\mathrm{j}f)\ \right] - \left[\ \underline{X}_1(\mathrm{j}f),\ \ \underline{X}_2(\mathrm{j}f)\ \right]. \tag{11}$$

Hence, after considering dynamic properties of the used operational amplifiers, described by the transmittance (4), (6) and the input impedance (8), one obtains the following equations:

$$\left[\ \underline{\Delta}^d_{x1},\ \ \underline{\Delta}^d_{x2}\ \right]_a = \left[\ \underline{U}(\mathrm{j}f),\ \ \underline{I}(\mathrm{j}f)\ \right] \begin{bmatrix} -\dfrac{\mathrm{j}\frac{f}{f_T}K^2_{01}}{1+\mathrm{j}\frac{f}{f_T}K_{01}} & 0 \\ 0 & -\dfrac{\mathrm{j}\frac{f}{f_T}K^2_{02}R_N}{1+\mathrm{j}\frac{f}{f_T}K_{02}} \end{bmatrix}, \tag{12}$$

$$\left[\ \underline{\Delta}_{x1}^{d},\ \ \underline{\Delta}_{x2}^{d}\ \right]_b = \left[\ \underline{U}(\mathrm{j}f),\ \ \underline{I}(\mathrm{j}f)\ \right] \begin{bmatrix} -\dfrac{\mathrm{j}\frac{f}{f_T}K_{01}^2}{1+\mathrm{j}\frac{f}{f_T}K_{01}} & 0 \\ -\dfrac{\mathrm{j}\frac{f}{f_T}K_{01}^2 R_N}{1+\mathrm{j}\frac{f}{f_T}K_{01}} & -\dfrac{\mathrm{j}\frac{f}{f_T}K_{02}^2 R_N}{1+\mathrm{j}\frac{f}{f_T}K_{02}} \end{bmatrix}, \tag{13}$$

$$\left[\ \underline{\Delta}_{x1}^{d},\ \ \underline{\Delta}_{x2}^{d}\ \right]_c = \left[\ \underline{U}(\mathrm{j}f),\ \ \underline{I}(\mathrm{j}f)\ \right] \begin{bmatrix} -\dfrac{\mathrm{j}\frac{f}{f_T}K_{01}^2}{1+\mathrm{j}\frac{f}{f_T}K_{01}} & 0 \\ \dfrac{\mathrm{j}\frac{f}{f_T}K_{01}R_N}{\left(1+\mathrm{j}\frac{f}{f_T}K_{01}\right)\left(1+\mathrm{j}\frac{f}{f_T}\right)} & \dfrac{\mathrm{j}\frac{f}{f_T}R_N}{1+\mathrm{j}\frac{f}{f_T}} \end{bmatrix}. \tag{14}$$

Subscripts *a*, *b*, *c* in Eqs. (12) – (14) denote the adequate conditioning circuits presented in Fig. 2a-c respectively.

As a result of propagation of these errors by the reconstruction algorithm (1) one obtains the complex dynamic errors of voltage and current measurement on the impedance $\underline{Z}$, defined as a matrix equation

$$\left[\ \underline{\Delta}_{U}^{d},\ \ \underline{\Delta}_{I}^{d}\ \right] = \left[\ \underline{\tilde{U}}(\mathrm{j}f),\ \ \underline{\tilde{I}}(\mathrm{j}f)\ \right] - \left[\ \underline{U}(\mathrm{j}f),\ \ \underline{I}(\mathrm{j}f)\ \right]. \tag{15}$$

These errors can be determined after taking into account an appropriate transformation matrix in Eqs. (12) – (14). For the conditioning circuit shown in Fig. 2a, the transformation matrix is equal to

$$\mathbf{T}_a = \begin{bmatrix} \dfrac{1}{K_{01}} & 0 \\ 0 & \dfrac{1}{K_{02}R_N} \end{bmatrix}. \tag{16}$$

In case of application of the conditioning circuit illustrated in Fig. 2b, the transformation matrix can be presented as

$$\mathbf{T}_b = \begin{bmatrix} \dfrac{1}{K_{01}} & 0 \\ -\dfrac{1}{K_{02}} & \dfrac{1}{K_{02}R_N} \end{bmatrix}. \tag{17}$$

For the circuit with active I/V converter (Fig. 2c), the corresponding transformation matrix can be written in the form

$$\mathbf{T}_c = \begin{bmatrix} \dfrac{1}{K_{01}} & 0 \\ 0 & -\dfrac{1}{R_N} \end{bmatrix}. \tag{18}$$

Hence, the suitable vectors of complex dynamic errors of reconstructed voltage and current values are equal to:

$$\left[\underline{\Delta}_U^d, \quad \underline{\Delta}_I^d \right]_a = \left[\underline{U}(\mathrm{j}f), \quad \underline{I}(\mathrm{j}f) \right] \begin{bmatrix} -\dfrac{\mathrm{j}\frac{f}{f_T}K_{01}}{1+\mathrm{j}\frac{f}{f_T}K_{01}} & 0 \\ 0 & -\dfrac{\mathrm{j}\frac{f}{f_T}K_{02}}{1+\mathrm{j}\frac{f}{f_T}K_{02}} \end{bmatrix}, \tag{19}$$

$$\left[\underline{\Delta}_U^d, \quad \underline{\Delta}_I^d \right]_b = \left[\underline{U}(\mathrm{j}f), \quad \underline{I}(\mathrm{j}f) \right] \begin{bmatrix} -\dfrac{\mathrm{j}\frac{f}{f_T}K_{01}}{1+\mathrm{j}\frac{f}{f_T}K_{01}} & 0 \\ R_N\left(\dfrac{\mathrm{j}\frac{f}{f_T}K_{01}}{1+\mathrm{j}\frac{f}{f_T}K_{01}} - \dfrac{\mathrm{j}\frac{f}{f_T}K_{02}}{1+\mathrm{j}\frac{f}{f_T}K_{02}}\right) & -\dfrac{\mathrm{j}\frac{f}{f_T}K_{02}}{1+\mathrm{j}\frac{f}{f_T}K_{02}} \end{bmatrix}, \tag{20}$$

$$\left[\underline{\Delta}_U^d, \quad \underline{\Delta}_I^d \right]_c = \left[\underline{U}(\mathrm{j}f), \quad \underline{I}(\mathrm{j}f) \right] \begin{bmatrix} -\dfrac{\mathrm{j}\frac{f}{f_T}K_{01}}{1+\mathrm{j}\frac{f}{f_T}K_{01}} & 0 \\ \dfrac{\mathrm{j}\frac{f}{f_T}R_N}{\left(1+\mathrm{j}\frac{f}{f_T}K_{01}\right)\left(1+\mathrm{j}\frac{f}{f_T}\right)} & -\dfrac{\mathrm{j}\frac{f}{f_T}}{1+\mathrm{j}\frac{f}{f_T}} \end{bmatrix}. \tag{21}$$

For a diagonal transformation matrix and the conditioning circuit with two voltage channels with differential input (Fig. 2a), the reconstructed voltage and current signals depend only on one of the input signals; thus the corresponding PDFs are independent.

The value set of the quantization error $\Delta^q(t)$ of the sampling transducer can be described by a uniform distribution [9, 13]. For a two-channel sampling transducer one obtains the bivariate distribution of random vector of quantization error $[\Delta_{x1}^q(t), \Delta_{x2}^q(t)]$. In this paper the assumption is that sampling occurs simultaneously in both transducer channels. Propagation of this error by the reconstruction algorithm changes its probabilistic properties. Thus, the PDF of random vector $[\Delta_u^q(t), \Delta_i^q(t)]$ is a composition of error distributions $\Delta_{x1}^q(t)$, $\Delta_{x2}^q(t)$.

The resultant error of a single processing result of vector $[u, i]$ is characterized by the PDF resulting from the distribution composition of dynamic and quantization errors [9].

In order to determine the processing uncertainty of a single measurement result of voltage and current, a simulation experiment has been carried out. It was assumed that the dynamic parameters of operational amplifiers (the same for both channels of the sampling transducer) are equal to: $f_T = 2$ MHz, $K_{0i} = 1$. The analyzed impedance equal to $\underline{Z}_{sim} = (1000 - j1000)\ \Omega$ has been fed from a sinusoidal voltage source with amplitude $U_{Gm} = 5$ V and frequency $f = 1000$ Hz. To minimize errors introduced by the signal conditioning circuit it was assumed that the standard series resistor (Fig. 2a,b) and the static transresistance of the I/V converter (Fig. 2c) comes to $R_N = |\underline{Z}_{sim}|$. Moreover, one assumed that the input ranges of two 12-bit A/D converters correspond to the amplitudes of quantized waveforms. Simulations were repeated 100,000 times, randomizing the sampling instant of input waveforms (simultaneously in both transducer channels) from the population with uniform distribution in the range from 0 to T ($T = 1/f$). The results of this experiment in a form of bivariate histograms of dynamic error $[\Delta_u^d, \Delta_i^d]$, quantization error $[\Delta_u^q, \Delta_i^q]$ and resultant error $[\Delta_u^c, \Delta_i^c]$ of a single processing result of two-channel sampling transducer have been presented in Figs. 3 and 4.

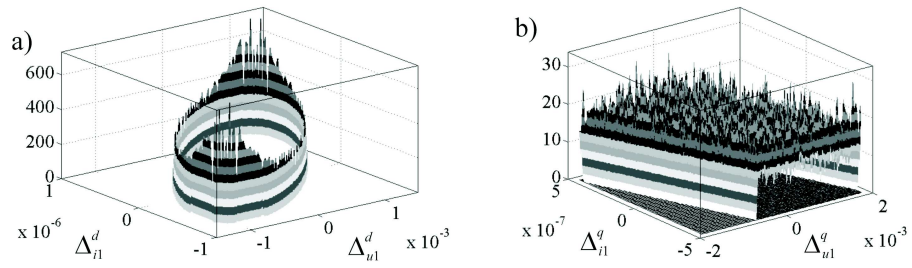

Fig. 3. Histograms of the single result error of the sampling transducer (for the circuit presented in Fig. 2b): dynamic error (a), quantization error (b).

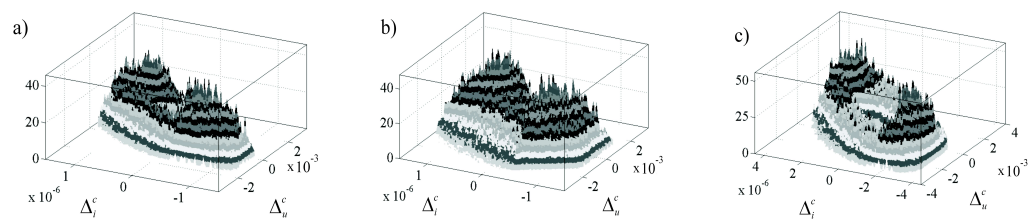

Fig. 4. Histograms of the resultant error of single sample processing in the two-channel sampling transducer for analysed conditioning circuits.

3. UNCERTAINTY ESTIMATION OF FINAL PROCESSING RESULT

To determine the impedance components values, when a linear, stationary and passive two-terminal network is stimulated with a sinusoidal wave with the specified frequency f, many processing algorithms of the reconstructed sample sequences of voltage $\{u(n)\}$ and current $\{i(n)\}$ signals are used [1–7]. One of the most popular methods of determining the impedance components consists in the application of impedance definition:

$$\underline{Z} = \frac{\underline{U}}{\underline{I}} = R + \mathrm{j}X = \frac{U_c I_c + U_s I_s}{I_c^2 + I_s^2} + \mathrm{j}\frac{U_s I_c - U_c I_s}{I_c^2 + I_s^2}, \tag{22}$$

where U_c, U_s, I_c, I_s, are the complex components of voltage and current.

To calculate these components the discrete Fourier transform (DFT) [4–5] is used. If the N samples of voltage and current are taken in a time corresponding to the total period multiple T of the feeding voltage generator, components of complex DFT for the fundamental harmonic f correspond to the values of voltage or current components:

$$\underline{U}^* = \frac{2}{N}\mathrm{DFT}[1, \mathbf{u}], \qquad \underline{I}^* = \frac{2}{N}\mathrm{DFT}[1, \mathbf{i}] \ , \tag{23}$$

where: $\mathrm{DFT}[k, \mathbf{u}] = \sum_{n=0}^{N-1} e^{-\mathrm{j}\frac{2\pi}{N}kn} u(n)$, $\mathrm{DFT}[k, \mathbf{i}] = \sum_{n=0}^{N-1} \mathrm{e}^{-\mathrm{j}\frac{2\pi}{N}kn} i(n)$, $\underline{U}^* = U_c - \mathrm{j}U_s$, $\underline{I}^* = I_c - \mathrm{j}I_s$.

The impedance components uncertainty calculated on the basis of the algorithm described by Eqs. (22) and (23) depends on the propagation result of N single sample processing PDFs of the two-channel sampling transducer by the processing algorithm as well as the uncertainty connected with the own error of the applied algorithm [8, 10, 13].

Estimation of the influence of the sampling transducer properties and the applied processing algorithm on the PDF of determined impedance components can be obtained with the simulation research method. For the transducer's parameter values presented in Chapter 2 the simulation experiment has been carried out, additionally taking into account that signals sampling in both processing channels has a frequency of $f_s = Nf$. Simulations were repeated $M = 100.000$ times, changing randomly the instant of taking the first sample of input waveforms (simultaneously in both transducer channels) in the range from 0 to T. As a result one obtained two matrixes containing M-elements random samples of N-elements output signals sequences of the A/D converters $\{x1(n)\}_m$ and $\{x2(n)\}_m$:

$$\mathbf{X}_1 = \begin{bmatrix} \{x_1(n)\}_1 \\ \vdots \\ \{x_1(n)\}_m \\ \vdots \\ \{x_1(n)\}_M \end{bmatrix}, \quad \mathbf{X}_2 = \begin{bmatrix} \{x_2(n)\}_1 \\ \vdots \\ \{x_2(n)\}_m \\ \vdots \\ \{x_2(n)\}_M \end{bmatrix}, \tag{24}$$

where $\{x_1(n)\}_m$ and $\{x_2(n)\}_m$ are the sequences containing signal samples obtained in m-trial.

Then, after application of the reconstruction algorithm the described components calculation algorithm has been used. The result of this calculation are M-element samples of the impedance components values. The resultant error of determining each of the components ΔR_m, ΔX_m has been calculated as follows

$$\underline{\Delta Z}_m = \Delta R_m + \mathrm{j}\Delta X_m = \underline{Z}_m - \underline{Z}_{sim}, \quad m = 1, \quad 2, \quad ..., \quad M, \tag{25}$$

where index m denotes the impedance value and error determined on its basis, obtained in m-trial, whereas $\underline{Z}_{sim}$ is the impedance value used for simulation calculation.

The error sets obtained this way have been arranged in order to get histograms. The bivariate histograms of resultant error $\Delta\underline{Z}$ for the analyzed structures of conditioning circuits are presented in Fig. 5.

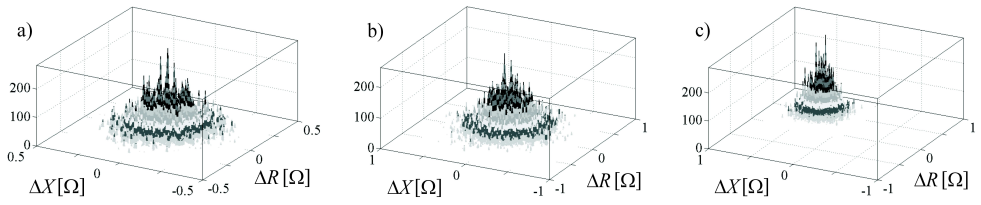

Fig. 5. Histograms of the resultant error of measured impedance $\Delta\underline{Z}$ for the algorithm (22), calculated by the simulation method (for $N = 20$ samples) for analyzed conditioning circuits.

Univariate PDFs for the real and imaginary component of error $\Delta\underline{Z}$ are the marginal PDFs towards each of the components. Histograms presenting such distributions can be obtained by arranging the sets of error results separately for each of the components. An example of such a histogram for the real component error is shown in Fig. 6.

Additionally, Fig. 7 illustrates empirical cumulative distribution functions (CDF) of the real component errors $G(\Delta R)$ for the analyzed algorithm (for $N = 20$ samples) in dependence on the applied conditioning circuit.

The CDFs of errors for the imaginary component $G(\Delta X)$, with regard to the impedance phase angle value ($\varphi = -\pi/4$), taken for simulation, do not differ significantly from the characteristics presented in Fig. 7. If the conditioning circuit with active

I/V converter is used (Fig. 2c), one obtains results burdened with a systematic error connected with the input impedance of the I/V converter. In the analyzed example $\underline{Z}_{in} \cong \mathrm{j}0,71\ \Omega$. This error can be eliminated by using an amplifier with differential input in the voltage measurement channel.

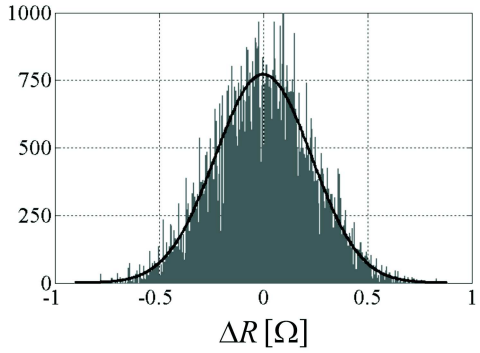

Fig. 6. Error ΔR histogram of the impedance real component for the algorithm (22), calculated by the simulation method for $N = 20$ samples. Probability density curve fitted for normal distribution with standard deviation $\sigma_R = \bar{s}_R$ is denoted with a solid line.

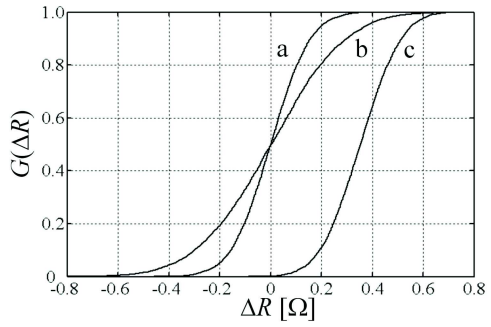

Fig. 7. Empirical cumulative distribution curves for impedance real component error $G(\Delta R)$ calculated for the conditioning circuits shown in Fig. 2a-c respectively.

The measurement result should be given together with its uncertainty estimation. If the PDF of the measurement result error is known, on the basis of the CDF of random variable $G(\Delta)$, one can determine the confidence interval Δ_α at confidence level α [11–12]. After elimination of possible systematic errors, for the symmetrical to zero PDF the confidence interval can be calculated from the equation

$$G(\Delta_\alpha) - G(-\Delta_\alpha) = \alpha. \tag{26}$$

For an error described with normal distribution, the confidence interval Δ_α determined on the basis of Eq. (26) corresponds to the expanded uncertainty U with the

coverage factor k_α. Table 1 shows the values of confidence intervals $\Delta_\alpha(R)$ (at confidence level $\alpha = 0,95$) determined on the grounds of (26) with the expanded uncertainty values for $k_\alpha = 2$. To estimate the uncertainty $u(R)$ the experimental standard deviation $\bar{s}_R$ has been applied [14].

Table 1. Confrontation of confidence intervals $\Delta_\alpha(R)$ at confidence level $\alpha = 0,95$ and expanded uncertainty $U(R) = 2u(R)$ for conditioning circuits under test.

Conditioning circuit	$N = 4$		$N = 20$		$N = 100$	
	$U(R)$	$\Delta_\alpha(R)$	$U(R)$	$\Delta_\alpha(R)$	$U(R)$	$\Delta_\alpha(R)$
Fig. 2a	0,563	0,541	0,247	0,244	0,111	0,110
Fig. 2b	1,036	0,998	0,462	0,449	0,208	0,205
Fig. 2c	0,565	0,544	0,249	0,244	0,108	0,106

4. CONCLUSIONS

In this paper the influence of the structure of signal conditioning circuits on the measurement uncertainty of impedance components has been presented. As a result of application of the Monte Carlo method, bivariate histograms of dynamic and quantization error for two-channel sampling transducer have been obtained. The resultant error of a single processing result of such a converter is characterized by the bimodal PDF. As a result of such an error propagation by the reconstruction algorithm, PDFs with different properties are obtained (Fig. 4). The application of the impedance components determining algorithm for N-element sequences of such processing results enables to calculate impedance component values. The measurement errors of these components, independently on the applied conditioning circuit, are characterized by the distribution which is similar to bivariate normal distribution (Fig. 5). It enables the calculation of confidence intervals on the basis of the uncertainty determined by method A and an appropriate coverage factor [14]. According to the results of the comparison of confidence intervals and expanded uncertainty (Table 1) as well as diagrams of empirical CDFs of errors (Fig. 7), the conditioning circuit with single-ended voltage inputs (Fig. 2b) for the same processing channel parameters is characterized by almost twice as high uncertainty value as the rest of the analysed circuits. Simultaneously, on the basis of the research, one can draw the conclusion that the application of the active I/V converter (Fig. 2c) causes systematic error of the impedance component measurement.

REFERENCES

1. Angrasani L., Ferrigno L.: *Reducing the uncertainty in real-time impedance measurements*, Measurement, 30, 2001, pp. 307–315.
2. Augustyn J.: *Algorithms of signals processing for immitance components measurement systems*, Metrology and Measurement Systems, no. 4 , 1999, pp. 223–230. (in Polish)

3. Augustyn J.: *A comparative evaluation of some LMS-based algorithms for calculating of impedance components in the sampling sensor instrument*, in: Proc. XVIIth IMEKO World Congress, Dubrovnik, Croatia, vol. TC4, 2003, pp.778–782.
4. Augustyn J.: *Algorithmic methods of impedance measurement*, Pomiary Automatyka Kontrola, no. 4, 2006, pp. 14–16. (in Polish)
5. Augustyn J.: *Algorithmic methods of impedance measurement*, Monografie, Studia, Rozprawy no. 53, Wyd. Politechniki Świętokrzyskiej, Kielce, 2006. (in Polish)
6. Augustyn J.: *Impedance measurement uncertainty added by algorithmic methods*, Pomiary Automatyka Kontrola, no. 10, 2007, pp. 3–6. (in Polish)
7. Ramos P. M., Fonseca da Silva M., Cruz Serra A.: *Low frequency impedance measurement using sine-fitting*, Measurement, no. 29, 2004, pp.89–96.
8. Jakubiec J.: *Metrological and signal description of properties of measurement data processing algorithms*, Materiały Konferencji "Podstawowe Problemy Metrologii", Ustroń, 14–17 maj 2006, Prace Komisji Metrologii Oddziału PAN w Katowicach, Seria: Konferencje no. 11, pp. 29–36. (in Polish)
9. Jakubiec J.: *System oriented mathematical model of single measurement result*, Metrology and Measurement Systems, no. 4, 2006, pp. 407–420.
10. Topór-Kamiński T.: *Experimental determination of own errors of the chosen DFT algorithm form*, Materiały Konferencji "Podstawowe Problemy Metrologii", Ustroń, 14–17 maj 2006, Prace Komisji Metrologii Oddziału PAN w Katowicach, Seria: Konferencje no. 11, pp. 341–352. (in Polish)
11. Cox M. G., Siebert B. R. L.: *The use of a Monte Carlo method for evaluating uncertainty and expanded uncertainty*, Metrologia, no. 43, 2006, pp. 178–188.
12. *Evaluation of measurement data – Supplement 1 to the "Guide to the expression of uncertainty in measurement" – Propagation of distributions using a Monte Carlo method*, Joint Committee for Guides in Metrology, September 2006.
13. Jakubiec J.: *Application of reductive interval arithmetic to uncertainty evaluation of measurement data processing algorithms*, Monografia no. 27, Wyd. Politechniki Śląskiej, Gliwice, 2002.
14. *Guide to the expression of uncertainty in measurement*, International Organization for Standarization, Geneva, 1995.